Biased Short Tract Repair of Palindromic Loop Mismatches in Mammalian Cells

Danielle G. Taghian, Heather Hough and Jac A. Nickoloff

Department of Cancer Biology, Harvard University School of Public Health, Boston, Massachusetts 02115

Manuscript received August 18, 1997
Accepted for publication November 13, 1997

ABSTRACT

Mismatch repair of palindromic loops in the presence or absence of single-base mismatches was investigated in wild-type and mismatch-binding defective mutant Chinese hamster ovary cells. Recombination intermediates with a maximum heteroduplex DNA (hDNA) region of 697 bp contained a centrally located, phenotypically silent 12-base palindromic loop mismatch, and/or five single-base mismatches. In wild-type cells, both loops and single-base mismatches were efficiently repaired (80–100%). When no other mismatches were present in hDNA, loops were retained with a 1.6–1.9:1 bias. However, this bias was eliminated when single-base mismatches were present, perhaps because single-base mismatches signal nick-directed repair. In the multiple marker crosses, most repair tracts were long and continuous, with preferential loss of markers in *cis* to proximal nicks, consistent with nicks directing most repair in this situation. However, ~25% of repair tracts were discontinuous as a result of loop-specific repair, or from segregation or short tract repair of single-base mismatches. In mutant cells, single-base mismatches were repaired less frequently, but the loop was still repaired efficiently and with bias toward loop retention, indicating that the defect in these cells does not affect loop-specific repair. Repair tracts in products from mutant cells showed a wide variety of mosaic patterns reflecting short regions of repair and segregation consistent with reduced nick-directed repair. In mutant cells, single-base mismatches were repaired more efficiently in the presence of the loop than in its absence, a likely consequence of corepair initiated at the loop.

MISMATCHED bases in DNA may arise from errors during DNA replication, from chemical modification of DNA, and during homologous recombination between nonidentical sequences. During replication, base misincorporation creates single-base mispairs, while DNA polymerase slippage on repeated sequences (*e.g.*, microsatellite sequences) may create mismatched loop structures. During recombination, heterologous point mutations, insertions and deletions can produce heteroduplex DNA (hDNA) with mismatched bases and loops. Mismatch repair deficient bacteria (Levinson and Gutman 1987) and yeast (Strand *et al.* 1993) display genome-wide microsatellite instability and mutator phenotypes, characterized by 100–1000-fold increases in spontaneous mutation rates. Microsatellite instability is also characteristic of some cancers (Boyer *et al.* 1995), and a similar mutator phenotype was observed at the microsatellite sequences in cells from patients with hereditary nonpolyposis colon cancer (HNPCC) (Aaltonen *et al.* 1993). Mutant mismatch repair genes cosegregate with HNPCC-associated loci (reviewed in Kolodner 1995), and mutations in these genes were also found in other tumor types (Boyer *et al.* 1995).

Both general and specific mismatch repair pathways exist in *Escherichia coli* (for review see Modrich 1991). The general pathway involves *mutHLS* and is well suited for correction of replication errors as it recognizes and repairs mismatches in newly synthesized, unmethylated DNA strands. In this system, MutS protein recognizes and binds to a mismatch and then forms a complex with MutL. Subsequently, MutH endonuclease nicks the unmethylated DNA strand, initiating excision/resynthesis tracts hundreds to thousands of bases long. Very short patch mismatch repair systems are mismatch specific. These involve *mutT* or *mutY*, function independently of the methylation state of the DNA, and are specific for G-T → G-C and G-A → G-C repair, respectively. *E. coli* correct most single-base mismatches and small loops (<4 bases) efficiently, but C-C and larger loop mismatches are corrected only as part of a tract initiated by another mismatch (Carraway and Marinus 1993).

In *Saccharomyces cerevisiae* and mammalian cells, analogous processes and protein homologs to the *mutHLS* system have been identified. Two yeast proteins, Msh2p and Msh6p recognize and form a complex on mismatched bases. Pms1p and Mlh1p then bind to this complex, creating a substrate suitable for excision and resynthesis by other enzymes. Similar reactions are seen in human cells with GT binding protein (GTBP, an Msh6p homolog), and hPms2 (a Pms1p homolog) (Kolodner 1995). Mismatch-specific repair is less well characterized in eukaryotes, although G-T mismatches have been shown to be preferentially repaired to G-C (Wie-

Corresponding author: Jac A. Nickoloff, Department of Molecular Genetics and Microbiology, School of Medicine, University of New Mexico, Albuquerque, NM 87131.
E-mail: jnickoloff@salud.unm.edu

bauer and Jiricny 1989), and the identification of short patch repair tracts suggests that mismatch-specific repair pathways exist in yeast (Weng *et al.* 1996) and mammalian cells (Heywood and Burke 1990b; Steeg *et al.* 1990; Carroll *et al.* 1994).

The *in vitro* and *in vivo* correction of all possible single-base mismatches has been reported (Bishop and Kolodner 1986; Brown and Jiricny 1988; Holmes *et al.* 1990; Varlet *et al.* 1990; Thomas *et al.* 1991; Fang and Modrich 1993), and many studies have found differential repair efficiencies and biased repair in favor of particular bases. In yeast and mammalian cells, single-stranded loops are efficiently bound by mismatch repair proteins and/or repaired (Ayares *et al.* 1987; Weiss and Wilson 1989; Umar *et al.* 1994; Alani *et al.* 1995). Palindromic loops longer than 12 bases (thought to form stem-loop structures) are poorly repaired in yeast (Nag *et al.* 1989; Nag and Petes 1991), but mammalian studies have suggested that palindromic loops of 14 bp (Deng and Nickoloff 1994) and 34 bp (Bollag *et al.* 1992) are repaired efficiently.

In *E. coli*, repair bias can be strand dependent (*mutHLS* pathway) or mismatch dependent (*mutT* and *mutY* pathways). In mammalian cells, nicks and DNA methylation status were examined as possible factors influencing repair bias. In one study, methylation status and nicks were found to influence strand discrimination in African green monkey kidney CV-1 cells (Hare and Taylor 1985), and other studies indicated that nicks are strong signals for strand-specific mismatch repair in human cell extracts (Holmes *et al.* 1990; Fang and Modrich 1993; Umar *et al.* 1994). However, conflicting results were obtained by Heywood and Burke (1990b), who found that nicks did not control strand targeting in COS-7 cells. Weiss and Wilson (1989) proposed that large nonpalindromic loop mismatches are a stronger signal than a nick for strand targeting. In that study, the non-loop DNA strand was used as template twice as often as the loop strand, leading to preferential loss of single-stranded loops 25–247 bp in length.

A study with an extrachromosomal recombination system that creates hDNA in recombination intermediates flanked by nicks on opposite strands suggested that nicks direct repair of single-base mismatches, and analyses of recombination frequencies suggested that a 14-base palindromic loop may be recognized and repaired independently of nicks, with repair biased toward loop retention (Deng and Nickoloff 1994). In the present study, analysis of recombination products provided additional evidence for biased retention of palindromic loops; this bias is opposite of that seen for single-stranded loops (Weiss and Wilson 1987). When loops were flanked by single-base mismatches, no bias was observed, a result consistent with single-base mismatches signaling general repair directed from nicks. The nick-directed repair pathway was found to be reduced in cells with a defect in mismatch binding (likely due to mutation in the CHO homolog of *hMSH2*), but these mutant cells are proficient in biased loop- and A-G mismatch-specific repair.

MATERIALS AND METHODS

Plasmid DNA: Plasmids were constructed by standard procedures (Sambrook *et al.* 1989). A single-base change creating a unique *Cla*I site was introduced into pSV2neo (Southern and Berg 1982), producing pSV2neoC, then three single-base changes creating an *Eco*RV site were introduced immediately upstream of the *neo* coding region, producing pSV2neoE. A 10-bp *Spe*I linker was inserted into a filled-in *Bss*HII site in *neo* of pSV2neoE, creating pSV2neoS(B)E; the S(B) frameshift mutation inactivates *neo*. Eleven phenotypically silent single-base mutations, creating new restriction fragment length polymorphisms (RFLPs), were introduced into pneo (Nickoloff and Reynolds 1990) by four rounds of unique site elimination mutagenesis (Deng and Nickoloff 1992), producing pneo11 (Miller *et al.* 1997). All 11 RFLPs were transferred to pneoAn (Deng and Nickoloff 1994) by using a domain replacement procedure (Ray *et al.* 1994), creating pneoAn11, and *Eco*RV sites were introduced into pneoAn and pneoAn11 as above, creating pneoAnE and pneoAnE11. The *Hin*dIII site at the *neo*/pUC19 border of pneoAnE and pneoAnE11 was filled in to create unique *Nhe*I sites, producing pneoAnN and pneoAnN11, respectively. Twelve-bp *Xho*I linkers were inserted into the *Eco*RV sites of pSV2neoE, pSV2neoS(B)E, and pneoAnN11, creating plasmids pSV2neoX, pSV2neoS(B)X, and pneoAnN11X. Plasmids used in recombination assays are shown in Figure 1A. To reduce effects from nonspecific nicks, plasmid DNAs used in recombination assays were prepared using an acidic phenol extraction procedure that produces >90% supercoiled DNA (Wang and Rossman 1994).

Cell culture and recombination assays: CHO cells were cultured as described previously (Nickoloff and Reynolds 1990; Taghian and Nickoloff 1995). Plasmid DNAs linearized with appropriate restriction enzymes were purified by spin column chromatography (Nickoloff 1994), and 0.1–0.2 μg of each DNA were electroporated into 4×10^6 cells in a volume of 0.8 ml using a pulse of 300 V, 960 μF, and a 0.4-cm electrode gap. Cells were then transferred to 300 ml of prewarmed growth medium. Cell viability was determined by plating appropriate dilutions in nonselective medium, and the remaining cells were inoculated into six 24-well dishes for selection 24 hr later with G418 (1250 mg/ml, 50% active; GIBCO, Grand Island, NY). Cell viability was reduced by about 50% by electroporation. After 10–12 days of growth in selective medium, G418-resistant ($G418^r$) colonies were dispersed within the wells, expanded to confluence, and genomic DNA was prepared. Control plates used to calculate recombination frequencies (or transfection frequencies when only one plasmid was introduced) were stained with 1% crystal violet in 70% ethanol.

Analysis of recombinant products: Ten μg of genomic DNA were digested with *Eco*RI, which excises integrated recombinant plasmids (Figure 1D), and religated at low concentration (50 μg/ml) to favor recircularization of the excised plasmid over ligation to other DNA fragments. DNAs were precipitated, electroporated into recombination-defective *E. coli* strain HB101 cells (Miller and Nickoloff 1995) and transformants resistant to both ampicillin and kanamycin (amp^r kan^r) were identified. Typically, 75% of amp^r kan^r products had expected recombinant structures, and the RFLP markers in these were analyzed by using agarose gel electrophoresis. Other structures in rescued plasmids may have resulted from integration within the *Eco*RI fragment used in plasmid rescue,

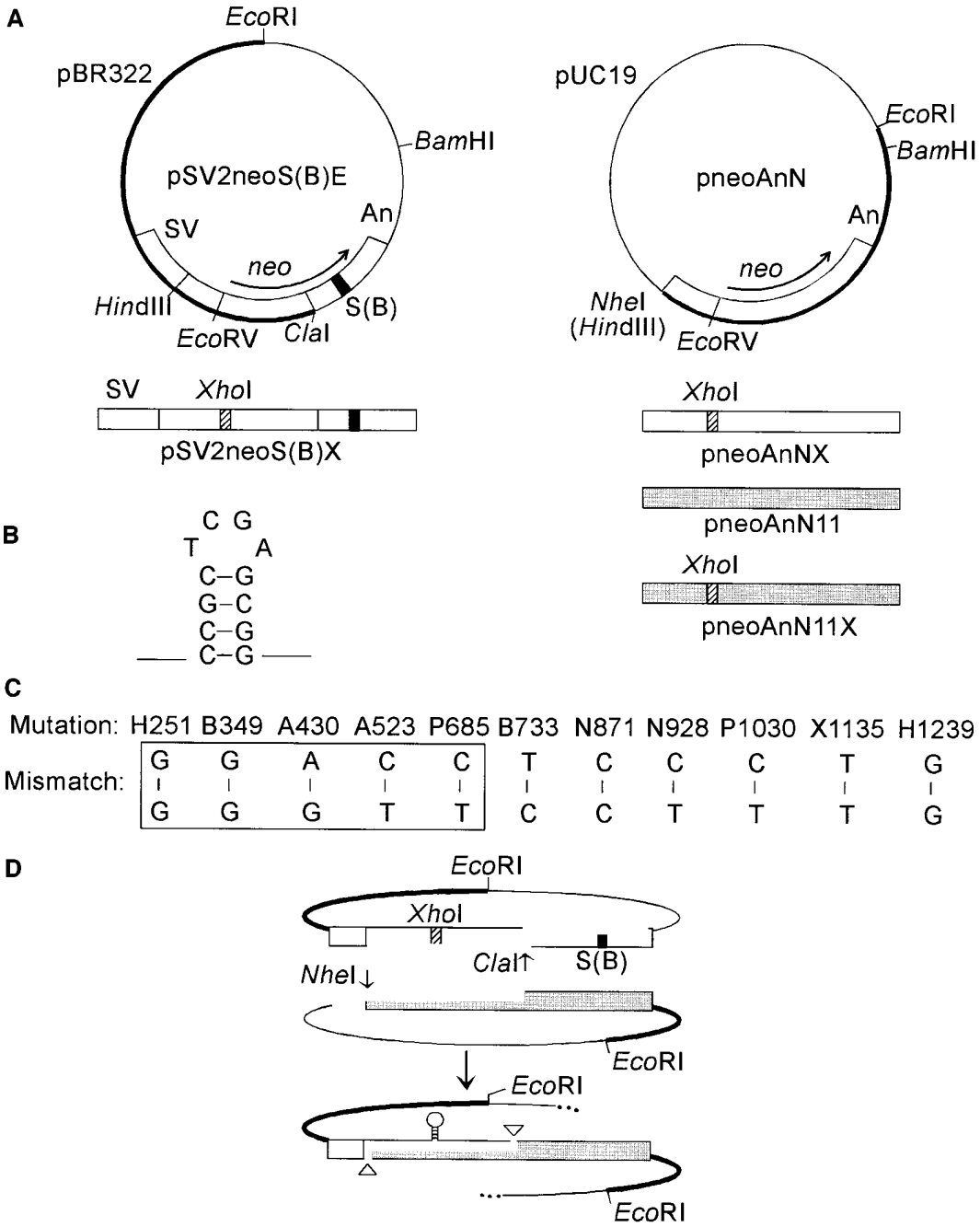

Figure 1.—System features. (A) Structures of recombination substrates. *neo* in pSV2neo derivatives is driven by the SV40 promoter and contains a frameshift mutation, S(B), indicated by the black bar. *neo* in pneoAn derivatives lacks a promoter, and some derivatives contain 11 silent single-base mutations (shading). Some substrates carry a 12-bp *Xho*I linker insertion (hatched bar), located at an engineered *Eco*RV site. This insertion is silent since it is upstream of the *neo* translation start site. *Cla*I and *Nhe*I are engineered sites used to linearize substrates for recombination assays, and are equidistant from the *Xho*I insertion (loop). *Eco*RI sites are used in plasmid rescue; heavy lines indicate regions isolated in rescued recombinants (see part D). (B) Predicted stem-loop structure for *Xho*I linker insertion. (C) RFLP mutations and corresponding mismatches formed in hDNA. Top bases listed are donated by pSV2neo derivatives; markers in hDNA are boxed. Numbers in marker names correspond to positions in *neo*, numbered from the *Hin*dIII site in pSV2neo. These mutations create the following restriction sites: H251 = *Hin*dIII, B349 = *Bam*HI, A430 = *Apa*I, A523 = *Apa*LI, P685 = *Pst*I, B733 = *Bam*HI, N871 = *Nru*I, N928 = *Nsi*I, P1030 = *Pml*I, X1135 = *Xba*I, H1239 = *Hin*dIII. (D) Extrachromosomal recombination as predicted by the SSA model, and rescue strategy. Single-stranded regions are degraded from *Cla*I and *Nhe*I DSBs, exposing complementary strands which anneal to produce a nonconservative crossover product with hDNA flanked by single-strand breaks in opposite strands (triangles) corresponding to DSB sites. In the example shown, hDNA contains RFLP markers (hatching) and a stem-loop mismatch. Recombinant molecules are rescued from genomic DNA by digesting with *Eco*RI, recircularizing with DNA ligase, and transforming into *E. coli.*

integration of pneoAn derivatives upstream of endogenous promoters, or from insertion of other genomic DNA fragments during the ligation step.

Segregation analysis: To measure repair efficiency, identical experiments to those described above were performed, except that at least six plasmid DNAs were rescued and analyzed from each transfectant. When all rescued plasmids had identical patterns it was taken as evidence for repair (0.03 confidence level). Mixed patterns were expected when one or more mismatches escape repair and segregate at the first round of replication following integration, producing a sectored colony. Segregation was sometimes scored using a PCR assay. Genomic DNA was amplified with primers complementary to the SV40 promoter (5′-GGCCTCTGAGCTATTCC AGA-3′) and to the 3′ end of *neo* (5′-CGAAATCTCGTGATGGCAGG-3′), yielding a 1.2-kbp product. Products with a single pattern for an RFLP were scored as having undergone repair, and mixed patterns were scored as segregation events. Because mixed patterns could also result if genomic DNA was prepared from independent transfectants, electroporated cells were distributed at low density (resulting in <3 colonies/24 wells). Under these conditions, a single well was unlikely to contain multiple transfectants ($P < 0.05$; Poisson distribution), thus ensuring that each colony arose from a single transfected cell. False sectors could also arise if a transfectant contained multiple copies of recombinant molecules. Thus, segregation analysis was performed only with transfectants containing one copy of an integrated recombinant molecule (about 50% of transfectants), as identified by Southern hybridization using a ^{32}P-labeled *neo* probe. Digestions with *Stu*I (one site in recombinants) and *Bst*XI (no site in recombinants) are diagnostic for tandem and non-tandem integrated molecules, respectively. Statistical analyses were performed using Fisher's exact tests.

RESULTS

Experimental design: Mismatch repair was studied using a two-plasmid extrachromosomal recombination assay that creates hDNA intermediates *in vivo* (Deng and Nickoloff 1994). Pairs of recombination substrates carried inactive *neo* heteroalleles. In pSV2neo derivatives, *neo* is driven by the SV40 promoter and inactivated by the S(B) linker frameshift mutation. pneoAn derivatives have functionally wild-type *neo* coding sequences, but lack a promoter. Some substrates carried phenotypically silent mutations, including a 12-bp palindromic *Xho*I linker insertion mutation upstream of the *neo* coding region, and/or eleven single-base changes at ~100-bp intervals that create RFLPs (Figure 1, A–C).

Recombination assays were performed by cotransfecting pairs of linearized plasmids into CHO cells and selecting for integrated neo$^+$ recombinants with G418. pSV2neo derivatives were linearized at a *Cla*I site located upstream of the S(B) frameshift, and pneoAn derivatives were linearized at an *Nhe*I site at the extreme 5′ end of the *neo* fragment. We and others (Lin *et al.* 1984; Wake *et al.* 1985; Anderson and Eliason 1986; Chakrabarti and Seidman 1986; Seidman 1987; Lin *et al.* 1990a; Deng and Nickoloff 1994; Miller *et al.* 1997) have shown that extrachromosomal recombination between heteroalleles linearized at appropriate sites yields products likely formed by single-strand annealing (SSA). This can produce intermediates with a hybrid DNA region flanked by nicks on opposite strands, corresponding to the original double-strand break (DSB) sites (Figure 1D). Conceivably, SSA can involve annealing between single strands exposed by either a 5′ to 3′ exonuclease or a 3′ to 5′ exonuclease. Although there was early evidence for 3′ to 5′ exonuclease activity in mouse L cells (Lin *et al.* 1987), several lines of evidence indicate that ends are processed by a 5′ to 3′ exonuclease. Studies in mouse ES cells and yeast provided clear evidence for 5′ to 3′ exonuclease acting at DNA ends (Henderson and Simons 1997; Huang and Symington 1993; Sun *et al.* 1991). In a study related to that reported here, evidence for 5′ to 3′ exonuclease activity mediating SSA in CHO cells was obtained in crosses predicted to yield individual single-base mismatches. Most single-base mismatches were repaired without bias, but crosses predicted to yield G-T mismatches via SSA mediated by 5′ to 3′ exonuclease activity showed a clear, strand-independent G-T → G-C repair bias (C. A. Bill, W. A. Duran, and J. A. Nickoloff, unpublished results). This bias is consistent with the well-known G-T → G-C repair systems in bacteria (Lieb 1991; Sohail *et al.* 1990) and mammalian cells (Brown and Jiricny 1988; Wiebauer and Jiricny 1989; Wiebauer and Jiricny 1990). Different mismatches are predicted for different exonuclease polarities, so a cross predicted to yield a G-T mismatch with a 5′ to 3′ exonuclease would yield a C-A mismatch if a 3′ to 5′ exonuclease was involved. There is no known system for biased repair of C-A mismatches, and we did not find a strand-independent bias for the two crosses predicted to produce C-A mismatches with a 5′ to 3′ exonuclease (or G-T mismatches with a 3′ to 5′ exonuclease).

In the present crosses, the two initiating DSBs flank a 697-bp region containing five markers predicted to produce single-base mismatches and/or a 12-base palindromic loop mismatch. Depending on the extent of exonuclease digestion, SSA intermediates may include more or less hDNA in the region between the DSBs, with maximum hDNA (697 bp) formed if exonuclease digestion extends from broken ends to (or past) DSB positions in recombining partners. Lesser digestion would produce less hDNA and annealed plasmids would contain flaps with 3′ ends; such flaps could be removed by homologs of yeast Rad1p/10p endonuclease (Ivanov and Haber 1995). Greater digestion would produce maximum hDNA flanked by single-stranded gaps that could be filled by extension of 3′ ends. Because a marker will occur in hDNA only if exposed in both duplexes, markers near one DSB are less likely to be included in hDNA because these are most distant from the other DSB. For simplicity, intermediates are shown with maximum hDNA flanked by single-strand nicks in Figures 1D and 2. Data presented below suggest that four of five markers occur in hDNA at similar rates ($\geq$50%), requiring 349–523 bases to be removed from either end.

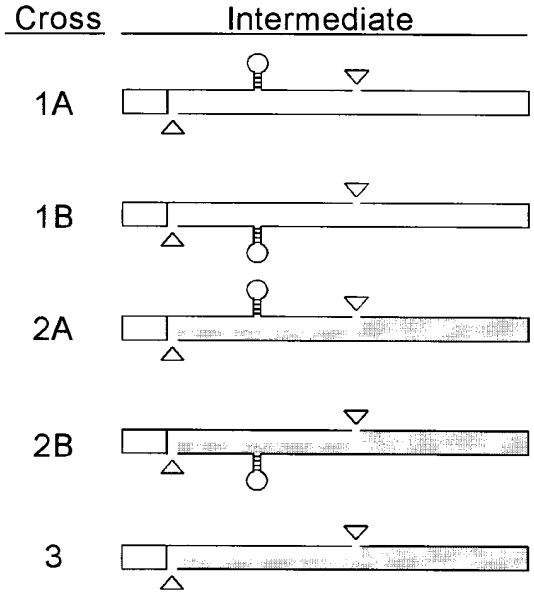

Figure 2.—Predicted recombination intermediates for five crosses. Symbols are as described in Figure 1D.

The fifth marker (P685) may occur in hDNA less often, which is not surprising since this requires the removal of at least 685 bases from the 5′ DSB. The loop mismatch is equidistant from the two DSBs and is therefore expected to occur in hDNA at maximum rates.

Mismatches are subject to repair either before or after integration. Mismatches in integrated recombinant molecules that escape repair will segregate during the next cell division and produce sectored colonies. As all markers are silent, there is no selective pressure for or against them. Recombinant products were rescued into *recA*$^-$ *E. coli*, or were PCR amplified, and all heteroallelic markers were scored to determine mismatch repair direction. Segregation analysis was performed on a subset of products to determine the efficiency of repair for each mismatch (see materials and methods). Crosses were performed in CHO K1c cells (wild-type), a mismatch-binding defective CHO line called clone B, and its wild-type parent, called MTCHO$^+$ (Branch *et al.* 1993).

Characterization of recombination substrates: Recombination substrates were electroporated into cells individually to determine background transfection frequencies (Table 1). pSV2neoS(B) yielded no G418^r colonies, indicating that the S(B) frameshift does not revert at detectable levels. Also, pSV2neoS(B) does not confer kan^r to *E. coli* transformants. Control CHO transfections with pSV2neo and pSV2neoX yielded G418^r colonies at similar levels, confirming the phenotypic silence of the *Xho*I linker insertion; the eleven single-base changes are also silent (Miller *et al.* 1997). pneoAn (with or without RFLPs) confers kan^r to *E. coli*. pneoAn plasmids introduced individually into CHO cells produced G418r colonies at frequencies 20–50-fold lower than in recombination experiments (Table 2). These rare G418^r colonies likely reflect integration of *neo* downstream of endogenous CHO promoters. Such products did not interfere with analysis of recombinants as they do not yield a rescued plasmid with the appropriate structure and are refractory to PCR amplification. Recombination frequencies were similar for all crosses in all three cell types (Table 2).

TABLE 1

Transfection frequencies with individual recombination substrates

Expt.[a]	Plasmid	Enzyme	Frequency ± ($\times 10^6$)[b]
1	pSV2neo	*Eco*RI	1180 ± 160
2	pSV2neoX	*Eco*RI	1260 ± 170
3	pSV2neoS(B)X	*Eco*RI	<0.03
4	pSV2neoS(B)X	*Cla*I	<0.03
5	pneoAnNX	*Nhe*I	0.4 ± 0.1
6	pneoAnN11X	*Nhe*I	0.5 ± 0.3

[a] All transfections performed in wild-type (K1c) cells.
[b] Transfection frequencies were calculated as the ratio of G418^r colonies per cell electroporated. Values are averages ± SD for three determinations. From 0.1 to 0.5 μg of each DNA were used in transfections; all frequencies are normalized to 0.1 μg of DNA.

Mismatch repair favors retention of palindromic loops: Previous analysis of recombination frequencies suggested that a 14-base palindromic loop mismatch was repaired with bias toward loop retention in CHO K1c cells (Deng and Nickoloff 1994). To obtain physical evidence for biased retention of palindromic loops, we performed crosses with a silent 12-base palindrome. In crosses 1A and 1B, the loop was present on opposite strands and was centrally located between the two DSBs (Figure 2). We reasoned that if nicks alone were directing the repair of the loop, an equal ratio of loop retention:loss would be observed. Instead we found similar 1.6–1.9:1 biases in favor of loop retention for both wild-type CHO lines (Table 3; $P = 0.025$ for combined data for crosses 1A and 1B). Thus, loop repair bias is both nick- and strand-independent.

Single-base mismatches eliminate loop repair bias: To determine whether nearby mismatches influence the direction of loop repair, we performed two crosses in which hDNA included up to five single-base mismatches in addition to the loop (crosses 2A and 2B, Figure 2). In contrast to crosses with only the loop mismatch, equal loop retention and loss were observed in the presence of single-base mismatches, regardless of which strand contained the loop (Table 3). These results are consistent with the loop being repaired by a nick-directed mechanism signaled by single-base mismatches (see discussion).

Mismatch repair tracts are predominantly long and nick directed: Three crosses with multiple single-base

TABLE 2

Recombination frequencies in wild-type and mutant CHO cells

Expt.	Cross[a]	Cell type[b]	Plasmid 1/*Cla*I	Plasmid 2/*Nhe*I	Frequency ($\times 10^6$)[c]	n[d]
1	1A	K1c	pSV2neoS(B)X	pneoAnN	9.8	1
2	1B	K1c	pSV2neoS(B)C	pneoAnNX	26 ± 11	2
3	2A	K1c	pSV2neoS(B)X	pneoAnN11	16 ± 3	2
4	2B	K1c	pSV2neoS(B)C	pneoAnN11X	27	1
5	3	K1c	pSV2neoS(B)C	pneoAnN11	19	1
6	2B	MTCHO$^+$	pSV2neoS(B)C	pneoAnN11X	10	1
7	2B	clone B	pSV2neoS(B)C	pneoAnN11X	16	1
8	3	MTCHO$^+$	pSV2neoS(B)C	pneoAnN11	7.5	1
9	3	clone B	pSV2neoS(B)C	pneoAnN11	19	1

[a] Crosses are diagrammed in Figure 2; pSV2neo and pneoAn derivatives were linearized at *Cla*I and *Nhe*I sites, respectively.

[b] K1c and MTCHO$^+$ cells are mismatch repair proficient, clone B cells are mismatch repair deficient.

[c] Recombination frequencies were calculated as the ratio of G418^r colonies per cell electroporated. Values are averages ± range for experiments repeated twice. From 0.1 to 0.2 μg of each DNA were used in transfections; all frequencies are normalized to 0.1 μg of pSV2neo derivative.

[d] Number of repetitions.

mismatches in CHO K1c cells (crosses 2A, 2B, and 3) allowed an examination of mismatch repair tract lengths and structures. The SSA model predicts that markers downstream of the *Cla*I site (B733, N871, N928, P1030, X1135, and H1239) will not be included in hDNA. Consistent with this prediction and previous results (Miller *et al.* 1997), all products contained the pneoAn markers in this region. Continuous tracts were found in 75% of products (Figure 3, types 1–7). Among all products, marker patterns displayed gradients (Figure 4) consistent with mismatch conversion occurring as a function of distance along *neo*, with markers converting more often when proximal to a nick in *cis*. Although such gradients could also reflect frequencies of marker inclusion in hDNA as a function of distance along *neo*, data presented below suggest a significant component of mismatch repair. Most repair appeared to involve long tracts initiated from nicks since 60% of the continuous tracts were of maximal length (types 1 and 7). Tract spectra for crosses 2A and 2B were similar to that of cross 3 (Figure 3). Thus, single-base mismatches influence loop repair (Table 3), but the loop in crosses 2A and 2B had little influence on the repair of single-base mismatches in wild-type cells.

TABLE 3

Biased repair of palindromic loop mismatches

	Percent palindrome retention (n)[b]			
	Loop alone		Loop + SBMMs	
Strain[a]	Cross 1A	Cross 1B	Cross 2A	Cross 2B
K1c	65 (51)	63 (27)	50 (38)	53 (32)
MTCHO$^+$	—	62 (34)	—	52 (29)
Clone B	—	56 (32)	—	55 (29)

[a] K1c and MTCHO$^+$ are mismatch repair proficient; clone B is mismatch repair deficient.

[b] Percentage of products that retained palindrome; number of products tested given in parentheses; SBMMs, single-base mismatches.

Evidence for short tract repair: Although most products had continuous marker patterns consistent with long repair tracts, discontinuous patterns were found in 29% of products from crosses 2A and 2B in CHO K1c cells. Discontinuous patterns are best explained as resulting from hDNA repair. Although such tracts could result from short tract and/or partial repair, segregation analysis (described below) indicates that most result from short tract repair. Most of these products had a single discontinuity, but four (Figure 3, types 10, 17–19) had two discontinuities. Among cross 2A and 2B products with discontinuous tracts, the loop repaired independently of the two flanking markers 45% of the time (*i.e.*, its repair was not directed from a nick). Interestingly, there was a twofold bias toward loop retention among this subset of products, which is similar to the bias observed in the absence of single-base mismatches. Thus, biased, loop-specific repair contributed significantly to the production of discontinuous tracts in crosses 2A and 2B (Figure 3), suggesting a degree of loop repair independent of nicks even in the presence of single-base mismatches. Surprisingly, the loop and B349, though only 10 bp apart, were repaired independently in 17% of all products, indicating that palindromic loop repair tracts can be relatively short.

Differential loop and single-base mismatch repair efficiencies in mismatch-binding defective cells: Segregation analysis was performed for crosses 1B, 2B, and 3 in wild-type and mutant cells to determine rates of marker involvement in hDNA and repair efficiencies for the loop and single-base mismatches. The loop segregated

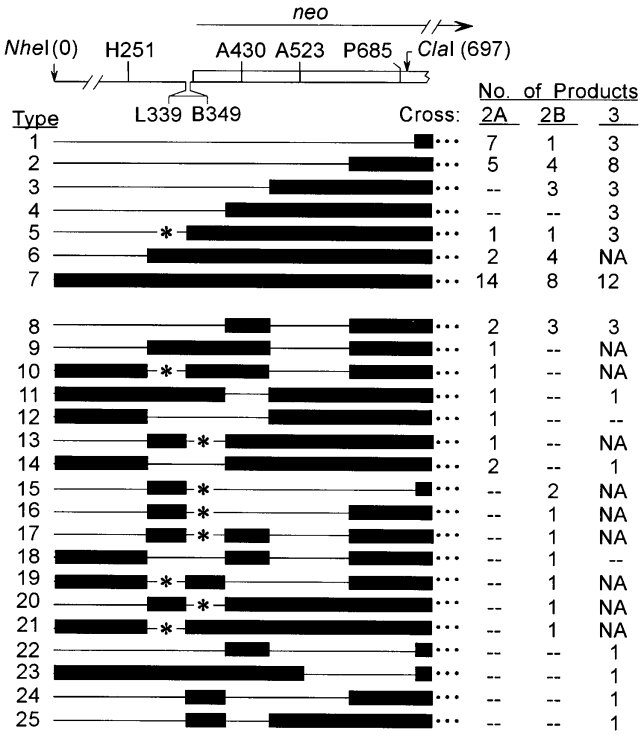

Figure 3.—Repair tract structures in products of crosses 2A, 2B and 3 in CHO K1c cells. A partial map of *neo* drawn to scale (top) shows the location of markers included in hDNA. Nicks in intermediates occur at *Nhe*I and *Cla*I sites at positions 0 and 697, as diagrammed in Figure 2. L339 (loop) and B349 are only 10 bp apart; this region is enlarged for clarity. Black bars indicate regions repaired toward sequence donated by pneoAn derivatives, thin lines indicate opposite repair; asterisks indicate products of crosses 2A and 2B in which L339 and B349 repaired independently. Tract types 1–7 are continuous repair tracts, likely originating from one or both nicks; types 8–25 are discontinuous. All products carry markers from pneoAn downstream of the *Cla*I site (three dots) as these are not included in hDNA. (--) indicates no products recovered; NA, not applicable as loop is not present.

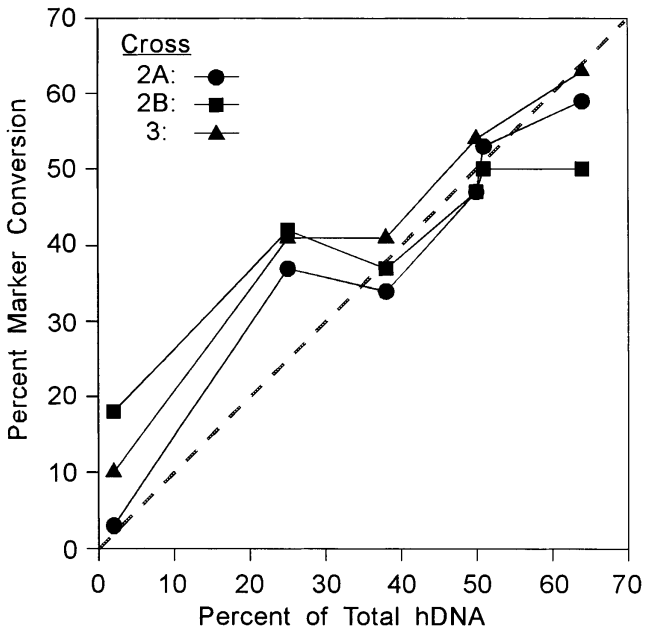

Figure 4.—Mismatch repair gradient. Percent marker conversion is plotted as a function of distance from the 3′ nick (converted to a percentage of total hDNA) for data shown in Figure 3. Dashed line indicates theoretical values if repair correlated perfectly to marker distances from nicks.

at low rates in both wild-type and mismatch defective cells, and in the presence or absence of single-base mismatches (Table 4 and Figure 5). In crosses 2B and 3, single-base mismatches also segregated at low rates in wild-type cells (0–15% of products had one or more segregating markers), but at high rates in mutant cells (35–53%; $P < 0.0002$ for combined cross 2B and 3 data). Thus, the defect in the mutant cells has no effect on loop repair, but markedly reduces repair of single-base mismatches.

Tract structures were determined for 69 products of crosses 2B and 3 in mutant cells. Thirty-eight had no segregating markers and the tract distributions for these products (not shown) were similar to those of wild-type cells (Figure 3). The remaining 31 products had one or more segregating markers, and were distributed among 29 different tract types (Figure 5). This wide variety of structures displayed striking mosaic patterns, reflecting frequent independent repair/segregation of adjacent markers. Together these results suggest that long-tract, nick-directed repair is reduced, but not eliminated in the mutant cells. Segregation was seen at all markers predicted to be in hDNA by the SSA model, providing evidence for hDNA formation via strand annealing in the region between the initiating DSBs.

As mentioned above, nick-directed repair would tend to reduce biases that arise from mismatch-specific repair. Thus, a clearer picture of loop repair bias can be gained by examining products in which the loop was repaired independently of repair tracts initiating at either nick. For cross 2B in mutant cells, there were nine such products (types 1–7 in Figure 5, plus two others that are not shown in which complete repair occurred) and seven of these nine products retained the loop

TABLE 4

Repair efficiencies of loops and single-base mismatches in wild-type and mutant cells

	Percent segregation (n)[b]		
Strains[a]	Cross 1B Loop only	Cross 2B Loop + SBMM	Cross 3 SBMM only
K1c + MTCHO$^+$	6 (47)	15 (26)	0 (12)
Clone B	10 (39)	35 (29)	53 (40)

[a] K1c and MTCHO$^+$ are mismatch repair proficient; clone B is mismatch repair deficient.

[b] Percentage of products that had one or more segregating markers; n, number of products tested; SBMM, single-base mismatches.

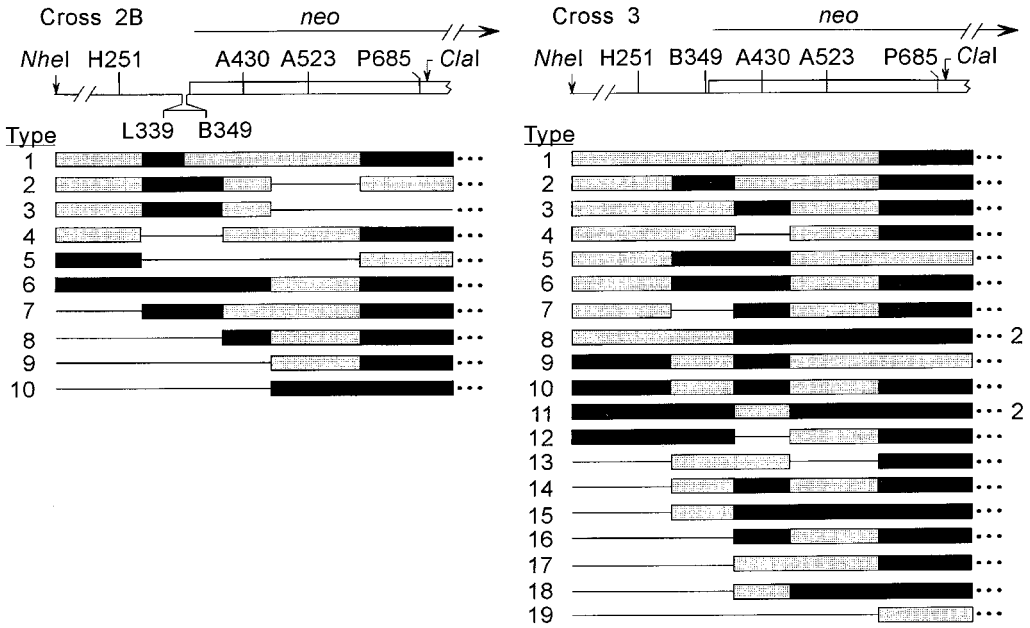

Figure 5.—Tract structures for products from clone B cells. Symbols are as described for Figure 3, with shaded bars indicating unrepaired mismatches. All product types shown were recovered once except types 8 and 11 from cross 3, which were recovered twice (indicated on right).

(3.5:1 bias). Thus, these mutant cells are competent in biased loop repair.

Minimum rates of hDNA formation: All markers except P685 showed significantly increased rates of segregation in mutant *vs.* wild-type cells (Figure 6; *P* values ranged from 0.0004 to 0.05), a clear indication of a mismatch repair defect in the mutant cells. As discussed above, the paucity of P685 segregations likely reflects a low rate of hDNA formation at this marker. For nonsegregating markers, continuous marker patterns could arise from nick-directed repair of hDNA or from intermediates with limited or no hDNA. Despite this uncertainty, hDNA (and hence repair) can be inferred for many nonsegregating markers in products with discontinuous patterns. This is true specifically when a marker is flanked by segregating markers and/or by markers repaired in opposite directions. Examples of such "non-nick-directed repair" for cross 3 include B349 in product types 2, 5, 6, 7, 11, and 12, and A430 in product types 3–7, 9, 10, 12, 14, and 16 (Figure 5). We can calculate minimum rates of hDNA formation for each marker from the sum of segregation events plus non-nick-directed repair events. Cross 3 in clone B cells displayed the highest segregation rate and hence provides the best estimate of the rate of hDNA formation at each marker. As shown in Figure 6, all markers except P685 were included in hDNA at minimum rates of ~50%.

Corepair of single-base and loop mismatches: In wild-type cells, all single-base mismatches showed similar segregation rates in the presence or absence of the loop (crosses 2B and 3; data not shown). In mutant cells, each of the four markers >88 bp from the loop also

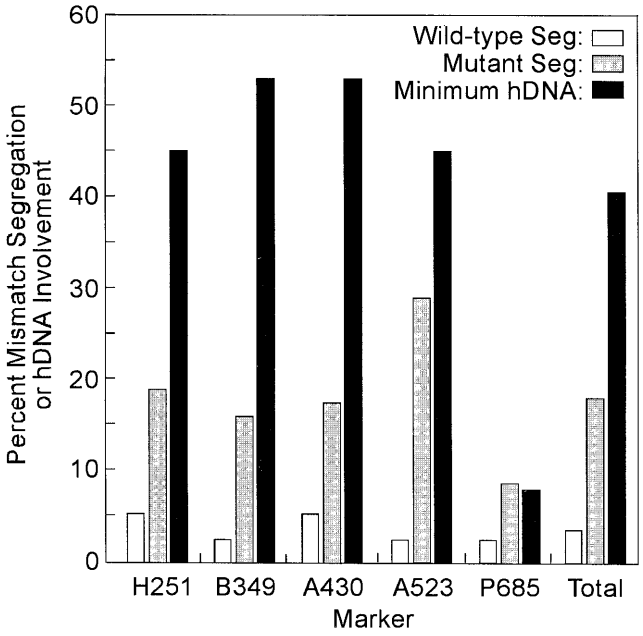

Figure 6.—Rates of segregation and hDNA involvement for individual single-base markers. Percent segregation in wild-type and mutant cells are shown with white and gray bars, respectively. Wild-type segregation values are for combined CHO K1c (crosses 2A, 2B and 3) and MTCHO$^+$ (crosses 2B and 3) products. Mutant segregation values are for clone B products (crosses 2B and 3). Minimum rates of hDNA involvement are shown as black bars; values are from cross 3 in clone B cells.

showed similar segregation rates in the presence or absence of the loop. The remaining marker, B349, located only 10 bp from the loop, segregated in mutant cells at a high rate in the absence of the loop (25%), but at a low rate in its presence (3.4%; $P = 0.013$). Thus, loop-specific repair in the mutant cells correlates with increased repair of B349, a likely consequence of corepair. Although dramatic effects were seen only at the close B349 marker, the presence of the loop also partially offset the difference in repair of single-base mismatches between wild-type and mutant cell lines (Table 4), suggesting that loop-specific repair sometimes leads to corepair of more distant markers.

DISCUSSION

Two prior studies indicated that the extrachromosomal recombination system used in the present study creates mismatches via SSA in a region defined by the positions of DSBs in recombination substrates, and that the resulting recombination intermediates are processed by an efficient, nick-directed repair mechanism (Deng and Nickoloff 1994; Miller *et al.* 1997). The observed segregation events at markers predicted to form mismatches (and only at these markers) provide clear evidence for the formation of hDNA intermediates. We exploited this system to examine the repair of a 12-base palindromic loop and/or five single-base mismatches. The plasmids used do not freely replicate and recombined DNAs integrate into the host cell genome either before or after mismatch repair of hDNA.

SSA is reduced in yeast *msh2* and *msh3* mismatch repair mutants. This effect is inversely proportional to lengths of shared homology, displaying a twofold reduction with 700 bp of shared homology (Sugawara *et al.* 1997), which is the maximum length of the annealed region in the present study. In contrast, recombination levels in the mismatch repair-deficient clone B cells were similar to levels in the wild-type CHO K1c and MTCHO$^+$ cells (Table 2). Any of a number of differences in the two studies could explain these contrasting results. For example, SSA in mammalian cells may proceed independently of mismatch repair functions, the effect may be influenced by allele linkage, or the two cell types may have different homology length thresholds.

Long tract repair: The present study and other (Desautels *et al.* 1990; Folger *et al.* 1985; Lehman *et al.* 1994; Miller *et al.* 1997) indicate that multiple markers in hDNA are usually repaired in continuous blocks. Biochemical evidence suggests that mammalian nick-directed mismatch repair is functionally similar to the excision-based *E. coli mutHLS* pathway (Fang and Modrich 1993). The conversion gradients we observed (Figure 4) are therefore consistent with long-tract mismatch repair initiating at nicks. With two nicks flanking hDNA, we can ask: how often (if ever) is repair initiated from both nicks of a single hDNA intermediate? Repair initiating from only one nick could produce continuous tracts in which all markers are repaired in a single direction. In the present study, and in a previous study (Miller *et al.* 1997), we found that a slight majority of products were of this type, suggesting that nick-directed repair tracts can extend the entire length of the hDNA region. In the vertebrate *Xenopus laevis*, a much greater fraction of products were of this type (Lehman *et al.* 1994), suggesting a greater repair processivity in *X. laevis* than in CHO cells.

Biased repair of palindromic loop mismatches: Insertion mutations produce loop mismatches in hDNA, and loops are also produced by DNA polymerase slippage. Nonpalindromic insertions produce single-stranded loops, whereas palindromic insertions of sufficient length produce stem-loop structures. The 12-bp palindromic insertion used in this study, despite being relatively short, would produce a stem with only G-C base pairs (Figure 1B) and is predicted to form a stable stem-loop structure ($\Delta G = -5.3$ kcal/mol; Oligo 5.0, National Biosciences, Plymouth, MN).

To study repair of loops without bias from nicks, we engineered substrates such that nicks on opposite DNA strands were equidistant from the loop. Several lines of evidence from this and earlier studies indicate that loops are repaired efficiently and independently of nicks. Previous measurements of recombination frequencies suggested biased retention of a frameshift mutation predicted to produce a 14-base palindromic loop mismatch (Deng and Nickoloff 1994). The present study of repair by physical analysis of markers in recombination products provides additional evidence for a significant bias toward loop retention when the loop is the only mismatch present in hDNA. However, because nicks are likely to direct some loop repair, and this would tend to produce equal loop retention and loss, a stronger bias may be found in the absence of nicks. Loop repair bias was eliminated when loops were flanked by single-base mismatches. Analogous corepair is seen in *E. coli* and yeast (Carraway and Marinus 1993; Petes *et al.* 1991; Weng and Nickoloff 1997). However, a 1.5:1 bias toward loop retention was evident even in the presence of single-base mismatches among those products in which the loop was clearly not repaired from either nick (Figure 3, crosses 2A and 2B, product types 9–21). Using an intrachromosomal recombination system to detect hDNA, Bollag *et al.* (1992) similarly found preferential retention of a 34-base palindromic loop in mouse Ltk$^-$ cells, suggesting that efficient, biased repair of palindromic loops is independent of sequence context and may be general for mammalian cells.

Contrasting results have been obtained for repair of single-stranded loops in mammalian cells. Although single-stranded loops of varying sizes are repaired efficiently, there is a 2:1 bias against loop retention (Weiss and Wilson 1987). Nicks had a minor effect on strand discrimination for biased repair of long (25–57 base)

single-stranded loops in monkey CV-1 cells (Weiss and Wilson 1989), but repair of a 5-base loop was efficient and nick-directed (*i.e.*, independent of loop location) in human cell extracts (Umar *et al.* 1994). In the absence of nicks, repair *in vitro* of a 5-base loop was inefficient, but there remained a strong (7:1) bias against this loop among products that did undergo repair (Umar *et al.* 1994). Similarly, repair of juxtaposed single-stranded loops without adjacent nicks in monkey cells favored retention of the smaller loop (Ayares *et al.* 1987). The opposite repair bias for palindromic and single-stranded loops provides evidence that the palindromic insertions we studied actually form stem-loop structures as predicted from biophysical considerations. The opposite repair biases also suggest that loop structure is an important determinant of both loop recognition and repair direction, and that there are distinct repair pathways for the two types of loops. Biochemical evidence in yeast that supports this notion includes the observations that Msh2p binds strongly to 12- and 14-base palindromic loops, but weakly to single-stranded loops (Alani *et al.* 1995), and the identification of a protein called IMR which binds 4–9 base single-stranded loops, but not palindromic loops (Miret *et al.* 1996). Weiss and Wilson (1989) suggested that single-stranded loops act as a stronger signal for repair than nearby nicks. Our data indicate that single-base mismatches override palindromic loop-specific repair, perhaps by recruiting nick-directed repair. It would appear that nick-directed repair, when enhanced by single-base mismatches, occurs faster than palindromic loop-specific repair.

Short tract repair of palindromic loops: Both prokaryotic and eukaryotic short tract repair systems are mismatch-specific. In *E. coli*, *mutT* and *mutY* pathways process specific base mismatches in short (<10 base) repair tracts (reviewed in Heywood and Burke 1990a; Kolodner 1995; Modrich 1991). While no short patch system has been identified in *S. cerevisiae*, there is evidence for a short patch pathway specific for C-C mispairs in *Schizosaccharomyces pombe* (Schar and Kohli 1993). Short tract repair in mammals includes a G-T system to deal with deaminated 5-methyl cytosine, and an A-G system involving *MYH* (a *mutY* homolog) (reviewed in Gallinari *et al.* 1997). Using HeLa cell extracts, Wiebauer and Jiricny (1990) showed that G-T → G-C repair involves removal of a single nucleotide. Short tract repair in mammalian cells was suggested by the observed independent repair of single-base mismatches separated by 20 bp in 60% of gene targeted products (Steeg *et al.* 1990), and by studies of transfected artificial hDNA substrates (Brown and Jiricny 1988; Heywood and Burke 1990b). Two studies demonstrated that non-palindromic loops separated by >200 bp were rarely corepaired, but complete corepair was seen when these markers were <60 bp apart (Ayares *et al.* 1987; Weiss and Wilson 1987). We found that a palindromic loop and a single-base mismatch separated by only 10 bp failed to corepair 17% of the time, indicating that palindromic loop repair tracts are sometimes very short.

Repair in mismatch-binding defective cells: Prior data indicated that the mutant CHO line, clone B, has several characteristics in common with mutants defective in mismatch repair, such as tolerance to alkylating agents, increased spontaneous mutagenesis and microsatellite instability, and defects in mismatch binding (Aquilina *et al.* 1994; Hess *et al.* 1994; Kat *et al.* 1993). In addition, clone B cell extracts fail to complement extracts of LoVo cells, which are defective in both alleles of *hMSH2*, and it was suggested that clone B and LoVo share this defect (Aquilina *et al.* 1994). Msh2-deficient mice also exhibit microsatellite instability, a mutator phenotype, and methylation tolerance (de Wind *et al.* 1995). Segregation of single-base mismatches was significantly higher in clone B cells than wild-type (Table 4), providing clear evidence for a mismatch repair defect. However, clone B cells are proficient at biased, palindromic loop-specific repair. In fact, loop-specific repair tended to increase overall repair of single-base mismatches in these cells, which is likely due to corepair initiated by loop-specific repair. Corepair was strong for the close B349 marker, but much less so for more distant markers, providing additional evidence that loop-specific repair often involves short tracts.

About half of the clone B products had one or more segregating markers and the other half had no segregating markers. Most marker patterns in products with no segregating markers were continuous and could have resulted from intermediates with extensive hDNA (by nick-directed repair of all markers), or from intermediates with limited or no hDNA. Extensive hDNA forms at least 50% of the time. If hDNA forms more often, our results would suggest that clone B cells perform some nick-directed repair, yielding continuous marker patterns. If hDNA forms only 50% of the time, our results would suggest that clone B cells perform essentially no nick-directed repair. In either case, reduced nick-directed repair may reflect reduced processivity, which could result from a defect in an exonuclease that acts at nicks, or from reduced signaling from mismatches. The mutation in clone B cells is likely subtle (*i.e.*, a single amino acid change) since clone B cells spontaneously revert to wild-type phenotype (Aquilina *et al.* 1989). If clone B cells are defective in Msh2 as suggested by Aquilina *et al.* (1994), a subtle change could alter the binding or signaling functions of the complexes that Msh2 forms with other proteins such as Msh3 or Msh6/GTBP. Since there is direct evidence for a mismatch binding defect in clone B cells (Aquilina *et al.* 1994), a reasonable model is that reduced mismatch binding reduces signals to the rest of the repair machinery, which in turn reduces repair processivity.

Our data would further suggest that Msh2 is not involved in loop-specific repair, which is consistent with the observation that although yeast Msh2p and Msh2p/

Msh6p bind to palindromic loop mismatches (Alani 1996; Alani *et al.* 1995), these mismatches often escape repair (Nag and Petes 1991; Nag *et al.* 1989). Finally, it would appear that yeast lack one or more components required for palindromic loop-specific repair. This may have a negligible effect in terms of the stability of the yeast genome, which is largely composed of unique sequences, but could have substantial effect on the stability of the large amount of repetitive DNA in mammalian genomes.

We thank M. Bignami for providing clone B and MTCHO$^+$ cells; E. M. Miller for constructing pneoAn11; D. Sweetser, J. Whelden, and N. Miselis for technical assistance; and C. Bill, D. Weaver, S. Powell, and M. Oettinger for helpful comments. This research was supported by grant CA54079 to J. Nickoloff from the National Cancer Institute, National Institutes of Health.

LITERATURE CITED

Aaltonen, L. A., P. Peltomaki, F. Leach, P. Sistonen, L. Pylkkanen *et al.*, 1993 Clues to the pathogenesis of familial colorectal cancer. Science **260:** 812–816.

Alani, E., 1996 The *Saccharomyces cerevisiae* Msh2 and Msh6 proteins form a complex that specifically binds to duplex oligonucleotides containing mismatched DNA base pairs. Mol. Cell. Biol. **16:** 5604–5615.

Alani, E., N.-W. Chi and R. D. Kolodner, 1995 The *Saccharomyces cerevisiae* Msh2 protein specifically binds to duplex oligonucleotides containing mismatched DNA base pairs and insertions. Genes Dev. **9:** 234–247.

Anderson, R., and S. L. Eliason, 1986 Recombination of homologous DNA fragments transfected into mammalian cells occurs predominantly by terminal pairing. Mol. Cell. Biol. **6:** 3246–3252.

Aquilina, G., A. Zijno, N. Moscufo, E. Dogliotti and M. Bignami, 1989 Tolerance to methylnitrosourea-induced DNA damageis associated with 6-thioguanine resistance in CHO cells. Carcinogenesis **10:** 1219–1223.

Aquilina, G., P. Hess, P. Branch, C. MacGeoch, I. Casciano *et al.*, 1994 A mismatch recognition defect in colon carcinoma confers DNA microsatellite instability and a mutator phenotype. Proc. Natl. Acad. Sci. USA **91:** 8905–8909.

Ayares, D., D. Ganea, L. Chekuri, C. R. Campbell and R. Kucherlapati, 1987 Repair of single-stranded nicks, gaps, and loops in mammalian cells. Mol. Cell. Biol. **7:** 1656–1662.

Bishop, D. K., and R. D. Kolodner, 1986 Repair of heteroduplex plasmid DNA after transformation into *Saccharomyces cerevisiae*. Mol. Cell. Biol. **6:** 3401–3409.

Bollag, R. J., D. R. Elwood, E. D. Tobin, A. R. Godwin and R. M. Liskay, 1992 Formation of heteroduplex DNA during mammalian intrachromosomal gene conversion. Mol. Cell. Biol. **12:** 1546–1552.

Boyer, J. C., A. Umar, J. I. Risinger, J. R. Lipford, M. Kane *et al.*, 1995 Microsatellite instability, mismatch repair deficiency, and genetic defects in human cancer cell lines. Cancer Res. **55:** 6063–6070.

Branch, P., G. Aquilina, M. Bignami and P. Karran, 1993 Defective mismatch binding and a mutator phenotype in cells tolerant to DNA damage. Nature **362:** 652–654.

Brown, T. C., and J. Jiricny, 1988 Different base/base mispairs are corrected with different efficiencies and specificities in monkey kidney cells. Cell **54:** 705–711.

Carraway, M., and M. G. Marinus, 1993 Repair of heteroduplex DNA molecules with multibase loops in *Escherichia coli*. J. Bacteriol. **175:** 3972–3980.

Carroll, D., C. W. Lehman, S. Jeong-Yu, P. Dohrmann, R. J. Dawson *et al.*, 1994 Distribution of exchanges upon homologous recombination of exogenous DNA in *Xenopus laevis* oocytes. Genetics **138:** 445–457.

Chakrabarti, S., and M. M. Seidman, 1986 Intramolecular recombination between transfected repeated sequences in mammalian cells is nonconservative. Mol. Cell. Biol. **6:** 2520–2526.

de Wind, N., M. Dekker, A. Berns, M. Radman and H. te Riele, 1995 Inactivation of the mouse Msh2 gene results in mismatch repair deficiency, methylation tolerance, hyperrecombination and predisposition to cancer. Cell **82:** 321–330.

Deng, W. P., and J. A. Nickoloff, 1992 Site-directed mutagenesis of virtually any plasmid by eliminating a unique site. Anal. Biochem. **200:** 81–88.

Deng, W. P., and J. A. Nickoloff, 1994 Mismatch repair of heteroduplex DNA intermediates of extrachromosomal recombination in mammalian cells. Mol. Cell. Biol. **14:** 400–406.

Desautels, L., S. Brouillette, J. Wallenburg, A. Belmaaza, N. Gusew *et al.*, 1990 Characterization of nonconservative homologous junctions in mammalian cells. Mol. Cell. Biol. **10:** 6613–6618.

Fang, W.-h., and P. Modrich, 1993 Human strand-specific mismatch repair occurs by a bidirectional mechanism similar to that of the bacterial reaction. J. Biol. Chem. **268:** 11838–11844.

Folger, K. R., K. Thomas and M. R. Capecchi, 1985 Efficient correction of mismatched bases in plasmid heteroduplexes injected into cultured mammalian cell nuclei. Mol. Cell. Biol. **5:** 70–74.

Gallinari, P., P. Neddermann and J. Jiricny, 1997 Short patch mismatch repair in mammalian cells, in *DNA Damage and Repair*, edited by J. A. Nickoloff and M. F. Hoekstra. Humana Press, Totowa, NJ (in press).

Hare, J. T., and J. H. Taylor, 1985 One role for DNA methylation in vertebrate cells is strand discrimination in mismatch repair. Proc. Natl. Acad. Sci. USA **82:** 7350–7354.

Henderson, G., and J. P. Simons, 1997 Processing of DNA prior to illegitimate recombination in mouse cells. Mol. Cell. Biol. **17:** 3779–3785.

Hess, P., G. Aquilina, E. Dogliotti and M. Bignami, 1994 Spontaneous mutations at aprt locus in a mammalian cell line defective in mismatch recognition. Som. Cell Mol. Genet. **20:** 409–421.

Heywood, L. A., and J. F. Burke, 1990a Mismatch repair in mammalian cells. Bioessays **12:** 473–477.

Heywood, L. A., and J. F. Burke, 1990b Repair of single nucleotide DNA mismatches transfected into mammalian cells can occur by short-patch excision. Mutat. Res. **236:** 59–66.

Holmes, J., Jr., S. Clark and P. Modrich, 1990 Strand-specific mismatch correction in nuclear extracts of human and *Drosophila melanogaster* cell lines. Proc. Natl. Acad. Sci. USA **87:** 5837–5841.

Huang, K. N., and L. S. Symington, 1993 A 5′-3′ exonuclease from *Saccharomyces cerevisiae* is required for in vitro recombination between linear DNA molecules with overlapping homology. Mol. Cell. Biol. **13:** 3125–3134.

Ivanov, E. L., and J. E. Haber, 1995 *RAD1* and *RAD10*, but not other excision repair genes, are required for double-strand break-induced recombination in *Saccharomyces cerevisiae*. Mol. Cell. Biol. **15:** 2245–2251.

Kat, A., W. G. Thilly, W.-H. Fang, M. J. Longley, G.-M. Li *et al.*, 1993 An alkylation-tolerant, mutator human cell line is deficient in strand-specific mismatch repair. Proc. Natl. Acad. Sci. USA **90:** 6424–6428.

Kolodner, R. D., 1995 Mismatch repair: mechanisms and relationship to cancer susceptibility. Trends Biochem. Sci. **20:** 397–401.

Lehman, C. W., S. Jeong-Yu, J. K. Trautman and D. Carroll, 1994 Repair of heteroduplex DNA in *Xenopus laevis* oocytes. Genetics **138:** 459–470.

Levinson, G., and G. A. Gutman, 1987 High frequencies of short frameshifts in poly-CA/TG tandem repeats borne by bacteriophage M13 in *Escherichia coli*. Nucleic Acids Res. **15:** 5523–5538.

Lieb, M., 1991 Spontaneous mutation at a 5-methylcytosine hotspot is prevented by very short patch (VSP) mismatch repair. Genetics **128:** 23–27.

Lin, F.-L., K. Sperle and N. Sternberg, 1984 Model for homologous recombination during transfer of DNA into mouse L cells: role for DNA ends in the recombination process. Mol. Cell. Biol. **4:** 1020–1034.

Lin, F.-L., K. Sperle and N. Sternberg, 1987 Extrachromosomal recombination in mammalian cells as studied with single- and double-stranded DNA substrates. Mol. Cell. Biol. **7:** 129–140.

Lin, F.-L., K. Sperle and N. Sternberg, 1990a Intermolecular recombination between DNAs introduced into mouse L cells is mediated by a nonconservative pathway that leads to crossover products. Mol. Cell. Biol. **10:** 103–112.

Lin, F.-L., K. Sperle and N. Sternberg, 1990b Repair of double-stranded breaks by homologous fragments during transfer of DNA into mouse L cells. Mol. Cell. Biol. **10:** 113–119.

Miller, E. M., and J. A. Nickoloff, 1995 *Escherichia coli* electrotransformation, pp. 105–113 in *Electroporation Protocols for Microorganisms*, edited by J. A. Nickoloff. Humana Press, Totowa, NJ.

Miller, E. M., H. L. Hough, J. W. Cho and J. A. Nickoloff, 1997 Mismatch repair by efficient nick-directed, and less efficient mismatch-specific mechanisms in homologous recombination intermediates in Chinese hamster ovary cells. Genetics **147:** 743–753.

Miret, J. J., B. O. Parker and R. S. Lahue, 1996 Recognition of DNA insertion / deletion mismatches by an activity in *Saccharomyces cerevisiae*. Nucleic Acids Res. **24:** 721–729.

Modrich, P., 1991 Mechanisms and biological effects of mismatch repair. Ann. Rev. Genet. **25:** 229–253.

Nag, D. K., and T. D. Petes, 1991 Seven-base-pair inverted repeats in DNA form stable hairpins *in vivo* in *Saccharomyces cerevisiae*. Genetics **129:** 669–673.

Nag, D. K., M. A. White and T. D. Petes, 1989 Palindromic sequences in heteroduplex DNA inhibit mismatch repair in yeast. Nature **340:** 318–320.

Nickoloff, J. A., 1994 Sepharose spin column chromatography: a fast, nontoxic replacement for phenol:chloroform extraction / ethanol precipitation. Mol. Biotech. **1:** 105–108.

Nickoloff, J. A., and R. J. Reynolds, 1990 Transcription stimulates homologous recombination in mammalian cells. Mol. Cell. Biol. **10:** 4837–4845.

Petes, T. D., R. E. Malone and L. S. Symington, 1991 Recombination in yeast, pp. 407–521 in *The Molecular and Cellular Biology of the Yeast Saccharomyces: Genome Dynamics, Protein Synthesis, and Energetics*, edited by J. R. Broach, J. R. Pringle and E. W. Jones. Cold Spring Harbor Laboratory Press, Cold Spring Harbor, NY.

Ray, F. A., E. M. Miller and J. A. Nickoloff, 1994 Efficient marker rescue and domain replacement without fragment subcloning. Anal. Biochem. **224:** 440–443.

Sambrook, J., E. F. Fritsch and T. Maniatis, 1989 *Molecular Cloning: A Laboratory Manual*, Cold Spring Harbor Laboratory Press, Cold Spring Harbor, NY.

Schar, P., and J. Kohli, 1993 Marker effects of G to C transversions on intragenic recombination and mismatch repair in *Schizosaccharomyces pombe*. Genetics **133:** 825–835.

Seidman, M. M., 1987 Intermolecular homologous recombination between transfected sequences in mammalian cells is primarily nonconservative. Mol. Cell. Biol. **7:** 3561–3565.

Sohail, A., M. Lieb, M. Dar and A. S. Bhagwat, 1990 A gene required for very short patch repair in *Escherchia coli* is adjacent to the DNA cytosine methylase gene. J. Bacteriol. **172:** 4214–4221.

Southern, P. J., and P. Berg, 1982 Transformation of mammalian cells to antibiotic resistance with a bacterial gene under control of the SV40 early region promoter. J. Mol. Appl. Genet. **1:** 327–341.

Steeg, C. M., J. Ellis and A. Bernstein, 1990 Introduction of specific point mutations into RNA polymerase II by gene targeting in mouse embryonic stem cells: evidence for a DNA mismatch repair system. Proc. Natl. Acad. Sci. USA **87:** 4680–4684.

Strand, M., T. A. Prolla, R. M. Liskay and T. D. Petes, 1993 Destabilization of tracts of simple repetitive DNA in yeast by mutations affecting DNA mismatch repair. Nature **365:** 207–208.

Sugawara, N., F. Paques, M. Colaiacovo and J. E. Haber, 1997 Role of *Saccharomyces cerevisiae* Msh2 and Msh3 repair proteins in double-strand break-induced recombination. Proc. Natl. Acad. Sci. USA **94:** 9214–9219.

Sun, H., D. Treco and J. W. Szostak, 1991 Extensive 3′-overhanging, single-stranded DNA associated with meiosis-specific double-strand breaks at the *ARG4* recombination initiation site. Cell **64:** 1155–1161.

Taghian, D. G., and J. A. Nickoloff, 1995 Electrotransformation of Chinese hamster ovary cells, pp. 115–121 in *Animal Cell Electroporation and Electrofusion Protocols*, edited by J. A. Nickoloff. Humana Press, Totowa, NJ.

Thomas, D. C., J. D. Roberts and T. A. Kunkel, 1991 Heteroduplex repair in extracts of human HeLa cells. J. Biol. Chem. **266:** 3744–3751.

Umar, A., J. C. Boyer and T. A. Kunkel, 1994 DNA loop repair by human cell extracts. Science **266:** 814–816.

Varlet, I., M. Radman and P. Brooks, 1990 DNA mismatch repair in Xenopus egg extracts: repair efficiency and DNA repair synthesis for all single base-pair mismatches. Proc. Natl. Acad. Sci. USA **87:** 7883–7887.

Wake, C. T., F. Vernaleone and J. H. Wilson, 1985 Topological requirements for homologous recombination among DNA molecules transfected into mammalian cells. Mol. Cell. Biol. **5:** 2080–2089.

Wang, Z., and T. G. Rossman, 1994 Large-scale supercoiled plasmid preparation by acidic phenol extraction. Biotechniques **16:** 460–463.

Weiss, U., and J. H. Wilson, 1987 Repair of single-stranded loops in heteroduplex DNA transfected into mammalian cells. Proc. Natl. Acad. Sci. USA **84:** 1619–1623.

Weiss, U., and J. H. Wilson, 1989 Effects of nicks on repair of single-stranded loops in heteroduplex DNA in mammalian cells. Som. Cell Mol. Genet. **15:** 13–18.

Weng, Y.-s., and J. A. Nickoloff, 1997 Evidence for independent mismatch repair processing on opposite sites of a double-strand break in *Saccharomyces cerevisiae*. Genetics **148:** 59–70.

Weng, Y.-s., J. Whelden, L. Gunn and J. A. Nickoloff, 1996 Double-strand break-induced gene conversion: examination of tract polarity and products of multiple recombinational repair events. Curr. Genet. **29:** 335–343.

Wiebauer, K., and J. Jiricny, 1989 In vitro correction of G-T mispairs to G-C pairs in nuclear extracts from human cells. Nature **339:** 234–236.

Wiebauer, K., and J. Jiricny, 1990 Mismatch-specific thymine DNA glycosylase and DNA polymerase β mediate the correction of G-T mispairs in nuclear extracts from human cells. Proc. Natl. Acad. Sci. USA **87:** 5842–5845.

Communicating editor: L. S. Symington